

UC Davis

UC Davis Previously Published Works

Title

Biosynthesis of neuroprotective melatonin is dysregulated in Huntingtons disease.

Permalink

<https://escholarship.org/uc/item/6tn1v7wg>

Journal

Journal of Pineal Research, 75(4)

Authors

Kim, Jinho

Li, Wei

Wang, Jingjing

et al.

Publication Date

2023-12-01

DOI

10.1111/jpi.12909

Peer reviewed



HHS Public Access

Author manuscript

J Pineal Res. Author manuscript; available in PMC 2024 December 01.

Published in final edited form as:

J Pineal Res. 2023 December ; 75(4): e12909. doi:10.1111/jpi.12909.

Biosynthesis of Neuroprotective Melatonin is Dysregulated in Huntington's Disease

Jinho Kim¹, Wei Li¹, Jingjing Wang¹, Sergei V. Baranov¹, Brianna E. Heath¹, Jiaoying Jia¹, Yalikus Suofu¹, Oxana V. Baranova¹, Xiaomin Wang¹, Timothy M. Larkin¹, William R. Lariviere¹, Diane L. Carlisle¹, Robert M. Friedlander¹

¹Neuroapoptosis Laboratory, Department of Neurological Surgery, University of Pittsburgh School of Medicine, Pittsburgh, PA, USA, 15213

Abstract

Huntington's disease (HD) is a progressive neurodegenerative brain disorder associated with uncontrolled body movements, cognitive decline, and reduced circulating melatonin levels. Melatonin is a potent antioxidant and exogenous melatonin treatment is neuroprotective in experimental HD models. In neurons, melatonin is exclusively synthesized in the mitochondrial matrix. Thus, we investigated the integrity of melatonin biosynthesis pathways in pineal and extrapineal brain areas in human HD brain samples, in the R6/2 mouse model of HD and in full length mutant huntingtin knock-in cells. Aralkylamine N-acetyltransferase (AANAT) is the rate limiting step enzyme in the melatonin biosynthetic pathway. We found that AANAT expression is significantly decreased in the pineal gland and the striatum of HD patients compared to normal controls. In the R6/2 mouse forebrain, AANAT protein expression was decreased in synaptosomal, but not non-synaptosomal, mitochondria and was associated with decreased synaptosomal melatonin levels compared to WT mice. We also demonstrate sequestration of AANAT in mutant-huntingtin protein aggregates likely resulting in decreased AANAT bioavailability. Paradoxically, *AANAT* mRNA expression is increased in tissues where AANAT protein expression is decreased, suggesting a potential feedback loop that is, ultimately unsuccessful. In conclusion, we demonstrate that pineal, extrapineal, and synaptosomal melatonin levels are compromised in the brains of HD patients and R6/2 mice due, at least in part, to protein aggregation.

Keywords

Huntington's disease; Melatonin; Mitochondria

Address correspondence to: friedlanderr@upmc.edu, Robert M. Friedlander, M.D., M.A., University of Pittsburgh School of Medicine, Department of Neurological Surgery, UPMC Presbyterian Hospital Suite B-449, 200 Lothrop Street, Pittsburgh, PA 15213, Tel: 412-647-6358.

Conflict of Interest: RF is Chair of the board of NeuBase Therapeutics. DLC previously served as a consultant for NeuBase Therapeutics. NeuBase Therapeutics did not provide funding for this project

INTRODUCTION

Huntington's disease (HD) is a progressive neurodegenerative disorder affecting basal ganglia and cortex, resulting in uncontrolled body movements, cognitive decline and premature death^{1,2}. HD is caused by a mutation in the *huntingtin* gene, which harbors an expanded number of CAG repeats encoding a toxic polyglutamine chain. Reduced plasma melatonin levels have been demonstrated in presymptomatic human HD patients, with disruption of circadian pineal melatonin biosynthesis occurring early in the disease^{3,4}. Melatonin is a potent antioxidant and has receptor-mediated neuroprotective properties^{5,6}. Exogenous melatonin is neuroprotective *in vivo* in acute and chronic neurodegenerative animal models, including in HD^{6,7}, amyotrophic lateral sclerosis (ALS)^{8–10}, Alzheimer Disease (AD)^{11–13}, Parkinson's Disease (PD)^{14–16}, multiple sclerosis (MS)¹⁷, and stroke^{18–20}. Melatonin-mediated neuroprotection results, at least in part, due to its ability to inhibit mitochondrial cytochrome c release and ensuing caspase-mediated cell death^{6,10,21}. Sequential caspase activation in R6/2 mice plays a functional role in mutant Huntingtin-mediated disease progression^{22,23}. Furthermore, mutant huntingtin expressing cells *in vitro* and *in vivo* mediate mitochondrial DNA release resulting in activation of cGAS/STING and neuroinflammatory pathways^{7,24}. We have recently demonstrated that melatonin inhibits mitochondrial DNA release and ensuing neuroinflammatory pathways in HD⁷. Autocrine melatonin pathways (i.e. mitochondrial melatonin release and binding to high affinity G-protein coupled melatonin receptors on the mitochondria) inhibit activation of cytotoxic cellular pathways²⁰. Thus, long-term reduction of melatonin synthesis may have detrimental consequences, thereby enhancing vulnerability by activating caspases and neuroinflammatory cascades of specific neuronal populations in HD patients.

Extrapineal melatonin is synthesized in a non-circadian mode in tissues throughout the body, where it has multiple autocrine and paracrine functions^{25,26}. Melatonin is detected in many organs including the brain, where concentrations are high compared to other tissues^{25,27}. mRNA for genes responsible for melatonin synthesis are expressed in the striatum and cortex²⁸. Furthermore, mitochondria—the site of highest free radical generation in the cell—have the highest melatonin concentration compared to other subcellular compartments²⁵, positing the loss of extrapineal mitochondrial melatonin as a potential contributor to neurodegeneration in HD. We demonstrated that melatonin is exclusively synthesized in neuronal mitochondria²⁰.

Therefore, we examined the integrity of the melatonin biosynthetic pathway in the pineal gland, cortex and striatum from human HD patients and brain tissues and isolated mitochondria from R6/2 mice and from full-length mutant huntingtin striatal cells. AANAT is the penultimate and rate-limiting enzyme in melatonin synthesis, and generates N-acetylserotonin from serotonin²⁹. Melatonin is then produced from N-acetylserotonin by acetylserotonin O-methyltransferase (ASMT)²⁸. In neurons, AANAT and ASMT are exclusively located in the mitochondrial matrix²⁰. To evaluate the etiology of mutant huntingtin-induced melatonin deficits, we determined the expression of *AANAT* and *ASMT* mRNA and protein *in vivo* in human and mouse specimens. We show that mutant huntingtin expression in human and mouse brain tissue results in a reduction of AANAT protein as well as a paradoxical increase of *AANAT* mRNA. Given that melatonin is protective *in vivo* in

models of HD^{6,30,31}, that there is a reduction of melatonin receptors in HD brains⁶, and that melatonin is broadly neuroprotective, the decreased availability of melatonin in neurons implicates melatonin as a relevant modulator of neuronal vulnerability in HD.

MATERIALS AND METHODS

Human brain samples

Acquisition and use of human brain tissues was performed with prior approval by the Committee for Oversight of Research and Clinical Training Involving Decedents of the University of Pittsburgh. Flash frozen, as well as fixed, human brain samples from male and female deceased HD patients and controls were obtained from the New York Brain Bank at Columbia University. Samples include pineal gland, cingulate gyrus, and putamen tissue samples from male and female HD patients (HD grade 1–4) and non-HD controls (Table 1).

Mice

All live vertebrate animal experiments were performed in compliance with the U.S. National Institutes of Health Guide for the Care and Use of Laboratory Animals and with approval by the Institutional Animal Care and Use Committee of the University of Pittsburgh. The R6/2 mouse model of HD was used, in which exon 1 of the human *HTT* gene is expressed with multiple CAG repeats, recapitulating many features of HD³². WT (B6CBA) and R6/2 mice offspring were produced by breeding in our colony, mating male R6/2 mice with female F1 B6CBA mice, and genotyping as previously described^{33,34}.

B6CBA mice were generated by breeding female C57BL/6J with male CBA/JR mice. CBA mice do not have spontaneous mutations of AANAT that are found in C57BL/6J³⁵, which has a naturally truncated AANAT protein; they also lack mutations in the ASMT gene³⁶.

Male WT and R6/2 littermates with polyQ repeat length between 145 and 155 Q were used in experiments. PolyQ repeat length was determined as previously³³.

Tissue lysis

Human and mouse brain tissues were lysed using published methods³³. Briefly, tissue was homogenized using a Teflon homogenizer and centrifuged at 1300 x g for three minutes. The supernatant was collected, and the pellet resuspended and homogenized again. This was repeated twice. The resulting pellet (cellular debris without homogenized tissue) was discarded, and supernatants obtained from each homogenization and centrifugation step were pooled for analysis.

Isolation of cerebral synaptosomal and non-synaptosomal mitochondria

Synaptosomal and non-synaptosomal mitochondria were isolated from fresh mouse brain tissues as previously described³³.

Due to the expected small yield from mouse brain tissues, four pooled forebrains of the same genotype were used for each mitochondria isolation.

Immunoblot analysis

Immunoblotting was used to identify and quantify proteins using the LiCor Odyssey system by Infrared fluorescence intensity. Briefly, 25 µg protein lysates were run on a PAGE gel, transferred to a PVDF-FL membrane and probed with the following primary antibodies: rabbit polyclonal anti-AANAT (1:2000 dilution, NIH, Supplementary Figure 1A); rabbit polyclonal anti-phospho-AANAT (1:2000, AB3439, Abcam; 1:200, bs-11448R, Bioss, Supplementary Figure 1B); rabbit polyclonal anti-ASMT (1:2000, bs-6961R, Bioss, Supplementary Figure 1C); mouse monoclonal anti- α -tubulin (1:1000, Sigma-Aldrich); mouse monoclonal anti-COX IV (1:5000, ab33985, Abcam). Secondary antibodies were goat anti-rabbit (1:20000, 926–32211, LiCor) and goat anti-mouse (1:20000, 926–68020, LiCor). Images of full blots for Figures 1–2 are shown in Supplementary Figures 2–7.

Immunostaining

To assess the intracellular localization of AANAT, WT and R6/2 mice were anesthetized, perfused with saline followed by 10% formalin, post-fixed overnight, and sequentially placed in 10% and 20% glycerol solution. Whole forebrains were then cut in 40 µm sections. Human HD patient and age matched control brain blocks were cut by using freeze sledge microtome in 40 µm sections. The free-floating sections were incubated with 10% horse serum for one hour then incubated with rabbit anti-AANAT (1:200, NIH) and mouse anti-mHTT (1:200, EM48, Chemicon, Sigma-Aldrich) or mouse anti-mitochondrially encoded cytochrome c oxidase II (1:500, MTCO2, Abcam ab3298) antibodies in PBS (pH 7) containing 0.05% Triton X-100 for 24–72 hours at 4°C. After three washes with PBS, slides were incubated with FITC-conjugated horse anti-mouse IgG (1:500, FI-2001, Vector Laboratories) and Alexa Fluor® 647-conjugated donkey anti-rabbit IgG (1:200, Jackson ImmunoResearch Laboratories) antibodies for two hours at room temperature. Sections were then mounted and cover slipped with mounting medium containing DAPI (Vectashield® H-1200, Vector Laboratories). Digital imaging was performed using an IX81 microscope (Olympus) equipped with an IX2-DSUA-SP confocal spinning disk and a 100X UPLSAPO objective (NA 1.40; Olympus) and UIS dichromatic mirror and appropriate emission filter sets (Olympus). Images were captured with a cooled charge-coupled device camera (Orca R2; Hamamatsu). Optical sections and 3D image reconstructions were performed using Metamorph software (Supplementary Figure 8, Molecular Devices). Images were captured at 0.2 µm intervals for 40 focal planes, and stacks were deconvoluted with an Autoquant software module by a constrained iterative algorithm. Orthoslice image panels were generated in NIH ImageJ using the View5D plugin (<https://imagej.net/Image5D>).

Melatonin concentration measurement

Mitochondria were isolated as described above. Diluted mitochondria were incubated in 600 µl chloroform for 1 hour with shaking at 500 rpm at 4°C. The chloroform extract (500 µl) was dried and the pellet was resuspended in 500 µl of PBS (pH 7.4). Protein concentration was measured by BCA protein assay (23225, Thermo Fisher Scientific). Mitochondrial protein (500 µg) was diluted in PBS (pH 7.4) to a final concentration of 1 mg/ml. Melatonin concentration was determined by ELISA kit (RE54021, IBL International) using the protocol provided by the manufacturer.

Quantitative reverse transcriptase PCR (qRT-PCR)

WT and R6/2 mouse brains were extracted at 6, 9, and 12 weeks of age, dissected into striatum and cortex and lysed for total RNA using a RNeasy kit (Qiagen). For mRNA, we used Nanodrop to check RNA quality using A260/A280, and A260/A320 before beginning with cDNA synthesis. Reverse transcription PCR (RT-PCR) was done using a high-capacity cDNA reverse transcription kit (Applied Biosystems). The cDNA products of RT-PCR were then amplified (BioRad CFX97 Touch™) using published validated primers for AANAT (5-GTCACTGGGCTGGTTTGAGG-3, 5-CTCCGGGCCTGTGTAGTGTC-3) and ASMT (5-GCAGCCTCCTGCTCTACCTG-3, 5-ACCTGTAGATGGCGGTGAAGG-3)³⁶ and mRNA expression was quantified using the 2^{-CT} method³⁷.

Experimental Design and Statistical Analysis

Statistical analyses were performed using Prism 6 software (GraphPad Software). Data are expressed as mean \pm standard error of the mean. For analysis of group differences between HD patients and controls or between R6/2 mice and WT mice, unpaired, two-tailed Student's *t*-tests were used to analyze the parametric data, unless otherwise indicated. Paired two-tailed *t*-tests were used to analyze synaptosomal and non-synaptosomal mitochondrial content of AANAT, phospho-AANAT, and AANAT mRNA. *P*-values less than 0.05 were considered statistically significant. Power analyses based on our previous and pilot studies with similar design indicate that a minimum of three biological replicates are necessary to detect significant group differences (with power of 0.80 and alpha 0.05) in protein expression (with minimum mean difference of 1.4 units, standard deviation of 0.3 units) and mRNA expression (minimum mean difference of 1.2 units, standard deviation of 0.5 units). Note that these power analyses are based on previous and pilot data and include pooling of samples in biological replicates as indicated for each assay above and in figure legends.

RESULTS

Specific melatonin biosynthetic enzymes are affected in the pineal gland and striatum of human HD patients

Bloodstream levels of melatonin are decreased in Huntington's Disease patients even prior to symptom onset^{3,4}. Since the pineal gland is the source of melatonin in the blood, we evaluated the key enzymes responsible for melatonin synthesis in the human pineal gland. AANAT is the rate limiting penultimate step in melatonin synthesis and ASMT is the final enzyme. We therefore evaluated the expression of AANAT and ASMT in the pineal gland of grade 3/4 HD patients and controls. The neuropathological HD classification has 5 grades, 0–4, whereby 0 has no pathological features of HD and 4 is the most severe classification. The grade assigned to each sample depends on striatal atrophy, striatal neuronal loss and degree of reactive astrogliosis^{38,39}. The rating of physical disability is highly correlated with neuropathological grading system. Grade 1 patients are ambulatory, in grade 2, ambulation is minimal. Grade 3 patients are confined to a wheelchair, and grade 4 patients are typically bed-ridden. In the pineal gland of grade 3/4 HD patients, AANAT protein expression is significantly lower (Fig. 1a; $t(4) = 5.39$, $p = 0.006$), and, paradoxically, expression of AANAT mRNA is increased (Fig. 1b; $t(11) = 2.19$, $p = 0.05$), compared to controls. In

contrast, no significant group differences were detected in the expression of *ASMT* protein (Fig. 1c; $t(5) = 0.20$, $p = 0.85$) or mRNA (Fig. 1d; $t(6) = 0.48$, $p = 0.65$) in the pineal gland.

It is unknown whether or not extra-pineal melatonin synthesis is regulated similarly to pineal melatonin synthesis; however, we previously demonstrated that melatonin is neuroprotective in HD mice^{6,20} and that melatonin is synthesized in neuronal mitochondria²⁰. Thus, we examined HD patient and control brain tissues for evidence of melatonin synthetic enzymes. We previously found that due to low AANAT brain concentrations, we only detect AANAT protein in enriched mitochondria samples²⁰. Hence, we used enriched brain mitochondria to evaluate AANAT levels in HD brain. In mitochondria-enriched striatum but not cortex samples of HD patients, a similar pattern of results is observed. AANAT protein expression is decreased (Fig. 1e; $t(5) = 4.82$, $p = 0.005$) and *AANAT* mRNA expression is increased (Fig 1f; $t(7) = 2.71$, $p = 0.03$) in the striatum of HD patients mitochondria fraction compared to controls.

Melatonin biosynthetic enzymes are similarly affected in extrapineal brain regions and synaptosomal mitochondria in the R6/2 mouse model of HD

We examined the degree to which R6/2 mice, a mouse expressing transgenic human exon 1 fragment with an expanded polyQ repeat⁴⁰, models HD patient phenotype with respect to *AANAT* mRNA. Similar to HD patients, in R6/2 mice expression of *AANAT* mRNA in the striatum and cortex is significantly greater than in WT mice at 6, 9, and 12 weeks of age (striatum: $t(8) = 2.32$, $p = 0.049$; $t(8) = 6.49$, $p < 0.001$; $t(12) = 5.24$, $p < 0.001$ respectively; and cortex: $t(8) = 2.43$, $p = 0.04$; $t(8) = 3.62$, $p = 0.007$; $t(12) = 3.02$, $p = 0.01$, respectively) (Fig. 2a,b). It is of interest that increased *AANAT* mRNA expression is seen as early as 6 weeks of age while the mice remain asymptomatic, suggesting that this is an early event in HD pathogenesis.

Since *AANAT* mRNA is encoded in the nucleus, transcribed in the cytosol, and its final subcellular localization is within the mitochondria matrix of neurons²⁰, it must be imported across the mitochondrial membrane. Since synaptosomal, but not non-synaptosomal, mitochondria have impaired mitochondrial protein import ability^{33,34}, and highly purified synaptosomal and nonsynaptosomal mitochondria can be obtained from mouse brain, we isolated synaptosomal and non-synaptosomal mitochondria from R6/2 whole forebrain samples. We found that brain synaptosomal mitochondria of R6/2 mice exhibit the same differences in melatonin biosynthetic enzymes as affected tissues from human HD patients. Total AANAT protein as well as phospho-AANAT, the active form of the enzyme, levels are significantly reduced in R6/2 mice compared to WT mice in synaptosomal mitochondria (Fig 2d; $t(2) = 9.60$, $p = 0.01$, paired t -test), but not non-synaptosomal mitochondria (Fig 2c; $t(2) = 0.28$, $p = 0.80$, paired t -test). Decreased AANAT protein corresponds with decreased melatonin levels in synaptosomal mitochondria compared to WT mice (Fig 2e; $t(4) = 2.91$, $p = 0.04$). As in human HD patient tissue samples, ASMT levels are unchanged between R6/2 and WT synaptosomal mitochondria (Fig 2f; $t(2) = 0.22$, $p = 0.84$, paired t -test). A specific deficit in synaptosomal mitochondria AANAT levels correlate with our findings that mutant huntingtin specifically affects synaptosomal mitochondria³³ resulting in enhanced synaptic

vulnerability, suggesting a role for melatonin deficit in enhancing synaptic vulnerability in HD.

Sequestration of AANAT protein in mHTT aggregates may underlie the discrepancy between mRNA and protein levels

AANAT mRNA is elevated in the pineal gland and striatum of HD patients and in R6/2 mice despite decreased AANAT protein detected in the same tissues compared to respective controls (Figs. 1, 2). Given this discrepancy, we evaluated the intracellular distribution of AANAT in R6/2 striatal cells (Fig 3a–b) and striatum of HD patients (Fig. 3c), and found AANAT colocalized with mHTT aggregates^{30,31}. Sequestration in aggregates may reduce the bioavailability of AANAT for melatonin biosynthesis and resulting in a compensatory increase in *AANAT* mRNA expression.

DISCUSSION

Melatonin has potent direct and indirect antioxidant properties. Melatonin is a free radical scavenger, and it also upregulates other antioxidant proteins such as MnSOD and Cu/ZnSOD, glutathione peroxidase (GPx) and Catalase (CAT)⁴¹. Additionally, melatonin has receptor-mediated antiapoptotic and antiinflammatory actions^{5–7}. Consistent with this, we recently reported increased oxidized protein content in R6/2 synaptosomal mitochondria compared to WT⁴². We now demonstrate that AANAT expression, the penultimate and rate-limiting enzyme in melatonin biosynthesis, but not ASMT, the final step in synthesis, is significantly reduced in the pineal gland of HD patients compared to controls. These results are in agreement with the reported reduction of plasma melatonin levels and reduced nighttime peaks in the blood of HD patients^{3,4} along with known suprachiasmatic nucleus (SCN) dysfunction^{43,44}.

In addition to synthesis in the pineal gland, it has been demonstrated the melatonin is made in the brain²⁶. Furthermore, in neurons, synthesis takes place in the mitochondria²⁰. Thus, we extended our studies beyond the pineal gland and we found increased *AANAT* mRNA expression but decreased AANAT protein in human HD striatum, R6/2 mouse cortex and striatum, and isolated R6/2 synaptosomal mitochondria from whole forebrain tissue compared to respective controls. Thus, we show for the first time that, in addition to decreased circulating plasma melatonin from the pineal gland, brain regions affected by HD are also impaired in their ability to synthesize melatonin. Reduced melatonin likely results from decreased AANAT protein levels in the mitochondria where melatonin biosynthesis occurs in neurons. Given the antioxidant properties of melatonin, reduced melatonin levels are expected to lead to increased oxidative stress in mHTT expressing neurons, resulting in cumulative oxidative damage of proteins and nucleic acids over time. Increased oxidative damage has been associated with aging and neurodegenerative diseases including HD^{45,46}.

We investigated the mechanisms that lead to AANAT protein insufficiency in neurons. Notably, although we found AANAT protein and *AANAT* mRNA expression affected in the cortex and whole forebrain of R6/2 mice, we did not observe significant differences in *AANAT* mRNA expression in cortical tissue between HD patients and controls. This may be due to the known clinical variability in the onset and location of cortical degeneration

and later onset of severe cognitive decline compared to motor impairment due to striatal neuronal degeneration in patients¹. This is in contrast to the aggressive and severe disease phenotype of the R6/2 mice, which includes early involvement of both the striatum and cortex⁴⁰.

Nonetheless, despite the differences between HD patients and the mouse model, it is clear that AANAT protein levels are decreased in neuronal mitochondria in the presence of mHTT. Our data demonstrating intracellular co-localization of AANAT with mHTT aggregates in striatal neurons suggests a mechanism for the HTT-mediated decrease in mitochondrial AANAT. These data suggest that reduced bioavailability of AANAT for melatonin synthesis in HD is due to adhesion/sequestration with mHTT polyglutamine aggregates, the pathogenic feature of mHTT.

Increased oxidative damage due to insufficient melatonin levels may lead to mitochondrial dysfunction observed as reduced mitochondrial membrane potential and reduced mitochondrial protein import. We recently showed that mitochondrial membrane potential is significantly lower, and mitochondrial protein import is impaired, in neurites of primary cortical neurons in culture of R6/2 mice compared to WT mice⁴². We showed that cumulative mitochondrial protein damage results in reduced mitochondrial membrane potential, impaired mitochondrial protein import and focal activation of the canonical apoptosis pathway in distal neurites in aged neurons and R6/2 neurons⁴². Furthermore, we showed that exogenous melatonin treatment is neuroprotective in R6/2 mice due to the inhibition of mitochondrial cytochrome c release and ensuing pro-apoptotic caspase activation^{6,10,21}. Our current data demonstrating decreased levels of AANAT in synaptosomal mitochondria, the same mitochondrial population known to have impaired mitochondrial protein import^{33,34,47}, suggests that impaired import may also play a role in decreased AANAT levels in HD.

Overall, the results indicate that in addition to HD patients having less neuroprotective plasma melatonin from the pineal gland, mitochondrial AANAT, the rate-limiting enzyme of melatonin biosynthesis, is less abundant in cerebral neurons. The overall reduction of melatonin levels in the brain may contribute to HD neuropathology.

Supplementary Material

Refer to Web version on PubMed Central for supplementary material.

Acknowledgements:

This work was supported by National Institute of Neurological Disorders and Stroke (NINDS) grants R01NS039324, R01NS051756 and R01NS100743 to R.M.F., and a generous gift from the David Scaife Family (DSF) Charitable Foundation to R.M.F. Human brain tissues were obtained from the New York Brain Bank at Columbia University/Taub Institute, supported by NIH Grant P50AG008702. We would like to thank Yue-Fang Chang for her statistical consultation and Ally Pickford for editorial assistance.

The data that support the findings of this study are available from the corresponding author upon reasonable request.

References

1. Morkl S, Muller NJ, Blesl C, et al. Problem solving, impulse control and planning in patients with early- and late-stage Huntington's disease. *European Archives of Psychiatry and Clinical Neuroscience*. 2016;266(7):663–671. [PubMed: 27372072]
2. Podvin S, Reardon HT, Yin K, Mosier C, Hook V. Multiple clinical features of Huntington's disease correlate with mutant HTT gene CAG repeat lengths and neurodegeneration. *J Neurol*. 2019;266(3):551–564. [PubMed: 29956026]
3. Aziz NA, Pijl H, Frolich M, et al. Delayed onset of the diurnal melatonin rise in patients with Huntington's disease. *J Neurol*. 2009;256(12):1961–1965. [PubMed: 19562249]
4. Kalliolia E, Silajdzic E, Nambron R, et al. Plasma Melatonin Is Reduced in Huntington's Disease. *Movement Disorders*. 2014;29(12):1511–1515. [PubMed: 25164424]
5. Reiter RJ, Tan DX, Manchester LC, El-Sawi M. Melatonin reduces oxidant damage and promotes mitochondrial respiration - Implications for aging. *Increasing Healthy Life Span: Conventional Measures and Slowing the Innate Aging Process*. 2002;959(1):238–250.
6. Wang X, Sirianni A, Pei Z, et al. The Melatonin MT1 Receptor Axis Modulates Mutant Huntingtin-Mediated Toxicity. *Journal of Neuroscience*. 2011;31(41):14496–14507. [PubMed: 21994366]
7. Jauhari A, Baranov SV, Suofu Y, et al. Melatonin inhibits cytosolic mitochondrial DNA-induced neuroinflammatory signaling in accelerated aging and neurodegeneration. *J Clin Invest*. 2020;130(6):3124–3136. [PubMed: 32182222]
8. Weishaupt JH, Bartels C, Polking E, et al. Reduced oxidative damage in ALS by high-dose enteral melatonin treatment. *J Pineal Res*. 2006;41(4):313–323. [PubMed: 17014688]
9. Jacob S, Poeggeler B, Weishaupt JH, et al. Melatonin as a candidate compound for neuroprotection in amyotrophic lateral sclerosis (ALS): high tolerability of daily oral melatonin administration in ALS patients. *J Pineal Res*. 2002;33(3):186–187. [PubMed: 12220335]
10. Zhang Y, Cook A, Kim JH, et al. Melatonin inhibits the caspase-1/cytochrome c/caspase-3 cell death pathway, inhibits MT1 receptor loss and delays disease progression in a mouse model of amyotrophic lateral sclerosis. *Neurobiology of disease*. 2013;55:26–35. [PubMed: 23537713]
11. Lahiri DK. Melatonin affects the metabolism of the beta-amyloid precursor protein in different cell types. *J Pineal Res*. 1999;26(3):137–146. [PubMed: 10231726]
12. Pappolla M, Bozner P, Soto C, et al. Inhibition of Alzheimer beta-fibrillogenesis by melatonin. *J Biol Chem*. 1998;273(13):7185–7188. [PubMed: 9516407]
13. Ali T, Kim MO. Melatonin ameliorates amyloid beta-induced memory deficits, tau hyperphosphorylation and neurodegeneration via PI3/Akt/GSK3 β pathway in the mouse hippocampus. *J Pineal Res*. 2015;59(1):47–59. [PubMed: 25858697]
14. Acuna-Castroviejo D, Coto-Montes A, Gaia Monti M, Ortiz GG, Reiter RJ. Melatonin is protective against MPTP-induced striatal and hippocampal lesions. *Life Sci*. 1997;60(2):PL23–29. [PubMed: 9000122]
15. Antolin I, Mayo JC, Sainz RM, et al. Protective effect of melatonin in a chronic experimental model of Parkinson's disease. *Brain Res*. 2002;943(2):163–173. [PubMed: 12101038]
16. Dabbeni-Sala F, Di Santo S, Franceschini D, Skaper SD, Giusti P. Melatonin protects against 6-OHDA-induced neurotoxicity in rats: a role for mitochondrial complex I activity. *Faseb Journal*. 2001;15(1):164–170. [PubMed: 11149904]
17. Lopez-Gonzalez A, Alvarez-Sanchez N, Lardone PJ, et al. Melatonin treatment improves primary progressive multiple sclerosis: a case report. *J Pineal Res*. 2015;58(2):173–177. [PubMed: 25546814]
18. Watson N, Diamandis T, Gonzales-Portillo C, Reyes S, Borlongan CV. Melatonin as an Antioxidant for Stroke Neuroprotection. *Cell Transplantation*. 2016;25(5):883–891. [PubMed: 26497887]
19. Wu YH, Feenstra MGP, Zhou JN, et al. Molecular changes underlying reduced pineal melatonin levels in Alzheimer disease: Alterations in preclinical and clinical stages. *Journal of Clinical Endocrinology & Metabolism*. 2003;88(12):5898–5906. [PubMed: 14671188]

20. Suofu Y, Li W, Jean-Alphonse FG, et al. Dual role of mitochondria in producing melatonin and driving GPCR signaling to block cytochrome c release. *Proc Natl Acad Sci U S A*. 2017;114(38):E7997–E8006. [PubMed: 28874589]
21. Wang X, Figueroa BE, Stavrovskaya IG, et al. Methazolamide and melatonin inhibit mitochondrial cytochrome C release and are neuroprotective in experimental models of ischemic injury. *Stroke*. 2009;40(5):1877–1885. [PubMed: 19299628]
22. Ona VO, Li M, Vonsattel JP, et al. Inhibition of caspase-1 slows disease progression in a mouse model of Huntington's disease. *Nature*. 1999;399(6733):263–267. [PubMed: 10353249]
23. Zhang Y, Ona VO, Li M, et al. Sequential activation of individual caspases, and of alterations in Bcl-2 proapoptotic signals in a mouse model of Huntington's disease. *J Neurochem*. 2003;87(5):1184–1192. [PubMed: 14622098]
24. Sharma M, Rajendrarao S, Shahani N, Ramírez-Jarquín UN, Subramaniam S. Cyclic GMP-AMP synthase promotes the inflammatory and autophagy responses in Huntington disease. *Proceedings of the National Academy of Sciences of the United States of America*. 2020;117(27):15989–15999. [PubMed: 32581130]
25. Venegas C, Garcia JA, Escames G, et al. Extrapineal melatonin: analysis of its subcellular distribution and daily fluctuations. *J Pineal Res*. 2012;52(2):217–227. [PubMed: 21884551]
26. Acuna-Castroviejo D, Escames G, Venegas C, et al. Extrapineal melatonin: sources, regulation, and potential functions. *Cell Mol Life Sci*. 2014;71(16):2997–3025. [PubMed: 24554058]
27. Sanchez-Hidalgo M, Guerrero Montavez JM, Carrascosa-Salmoral MD, Naranjo Gutierrez MD, Lardone PJ, Romero CAD. Decreased MT1 and MT2 melatonin receptor expression in extrapineal tissues of the rat during physiological aging. *J Pineal Res*. 2009;46(1):29–35. [PubMed: 18513209]
28. Stefulj J, Hortner M, Ghosh M, et al. Gene expression of the key enzymes of melatonin synthesis in extrapineal tissues of the rat. *J Pineal Res*. 2001;30(4):243–247. [PubMed: 11339514]
29. Falcon J, Besseau L, Fuentes M, Sauzet S, Magnanou E, Boeuf G. Structural and Functional Evolution of the Pineal Melatonin System in Vertebrates. *Trends in Comparative Endocrinology and Neurobiology*. 2009;1163:101–111.
30. Tunez I, Montilla P, Del Carmen Munoz M, Feijoo M, Salcedo M. Protective effect of melatonin on 3-nitropropionic acid-induced oxidative stress in synaptosomes in an animal model of Huntington's disease. *J Pineal Res*. 2004;37(4):252–256. [PubMed: 15485551]
31. Antunes Wilhelm E, Ricardo Jesse C, Folharini Bortolatto C, Wayne Nogueira C. Correlations between behavioural and oxidative parameters in a rat quinolinic acid model of Huntington's disease: Protective effect of melatonin. *European Journal of Pharmacology*. 2013;701(1):65–72. [PubMed: 23340221]
32. Mangiarini L, Sathasivam K, Seller M, et al. Exon 1 of the HD gene with an expanded CAG repeat is sufficient to cause a progressive neurological phenotype in transgenic mice. *Cell*. 1996;87(3):493–506. [PubMed: 8898202]
33. Yano H, Baranov SV, Baranova OV, et al. Inhibition of mitochondrial protein import by mutant huntingtin. *Nature neuroscience*. 2014;17(6):822–831. [PubMed: 24836077]
34. Yablonska S, Ganesan V, Ferrando LM, et al. Mutant huntingtin disrupts mitochondrial proteostasis by interacting with TIM23. *Proc Natl Acad Sci U S A*. 2019;116(33):16593–16602. [PubMed: 31346086]
35. Roseboom PH, Namboodiri MA, Zimonjic DB, et al. Natural melatonin 'knockdown' in C57BL/6J mice: rare mechanism truncates serotonin N-acetyltransferase. *Brain Res Mol Brain Res*. 1998;63(1):189–197. [PubMed: 9838107]
36. Kasahara T, Abe K, Mekada K, Yoshiki A, Kato T. Genetic variation of melatonin productivity in laboratory mice under domestication. *Proc Natl Acad Sci U S A*. 2010;107(14):6412–6417. [PubMed: 20308563]
37. Yeatts K Quantitative polymerase chain reaction using the comparative C q method. *Methods Mol Biol*. 2011;700:171–184. [PubMed: 21204034]
38. Rüb U, Vonsattel JPG, Heinsen H, Korf H-W. The Neuropathological Grading of Huntington's Disease (HD). In: *The Neuropathology of Huntington's Disease: Classical Findings, Recent*

- Developments and Correlation to Functional Neuroanatomy. Cham: Springer International Publishing; 2015:7–23.
39. Vonsattel J-P, Myers RH, Stevens TJ, Ferrante RJ, Bird ED, Richardson EP, Jr. Neuropathological Classification of Huntington's Disease. *Journal of Neuropathology & Experimental Neurology*. 1985;44(6):559–577. [PubMed: 2932539]
 40. Stack EC, Kubilus JK, Smith K, et al. Chronology of behavioral symptoms and neuropathological sequela in R6/2 Huntington's disease transgenic mice. *Journal of Comparative Neurology*. 2005;490(4):354–370. [PubMed: 16127709]
 41. Reiter RJ, Tan DX, Osuna C, Gatto E. Actions of Melatonin in the Reduction of Oxidative Stress. *Journal of Biomedical Science*. 2000;7(6):444–458. [PubMed: 11060493]
 42. Baranov SV, Baranova OV, Yablonska S, et al. Mitochondria modulate programmed neuritic retraction. *Proceedings of the National Academy of Sciences of the United States of America*. 2019;116(2):650–659. [PubMed: 30584104]
 43. Kuljis D, Kudo T, Tahara Y, Ghiani CA, Colwell CS. Pathophysiology in the suprachiasmatic nucleus in mouse models of Huntington's disease. *Journal of Neuroscience Research*. 2018;96(12):1862–1875. [PubMed: 30168855]
 44. Kuljis DA, Gad L, Loh DH, et al. Sex Differences in Circadian Dysfunction in the BACHD Mouse Model of Huntington's Disease. *PLoS One*. 2016;11(2):e0147583. [PubMed: 26871695]
 45. Dugan LL, Quick KL. Reactive oxygen species and aging: evolving questions. *Sci Aging Knowledge Environ*. 2005;2005(26):pe20. [PubMed: 15994214]
 46. Patten DA, Germain M, Kelly MA, Slack RS. Reactive oxygen species: stuck in the middle of neurodegeneration. *J Alzheimers Dis*. 2010;20 Suppl 2:S357–367. [PubMed: 20421690]
 47. Baranov SV, Jauhari A, Carlisle DL, Friedlander RM. Two hit mitochondrial-driven model of synapse loss in neurodegeneration. *Neurobiology of disease*. 2021;158:105451. [PubMed: 34298088]

SIGNIFICANCE STATEMENT

Huntington's disease (HD) is a progressive neurodegenerative brain disorder associated with uncontrolled body movements, cognitive decline, and in humans a decrease in circulating melatonin levels compared to healthy controls. Because melatonin is a potent antioxidant and is neuroprotective, we studied melatonin synthesis in human HD patients and mice that model HD. We found that levels of the rate-limiting melatonin biosynthetic enzyme aralkylamine N-acetyltransferase (AANAT), but not acetylserotonin O-methyltransferase (ASMT), are significantly decreased in HD human pineal gland, striatum, and cortex, and in HD mouse forebrain synaptosomal mitochondria. We also report that AANAT is present in mutant-huntingtin aggregates, likely reducing its bioavailability.

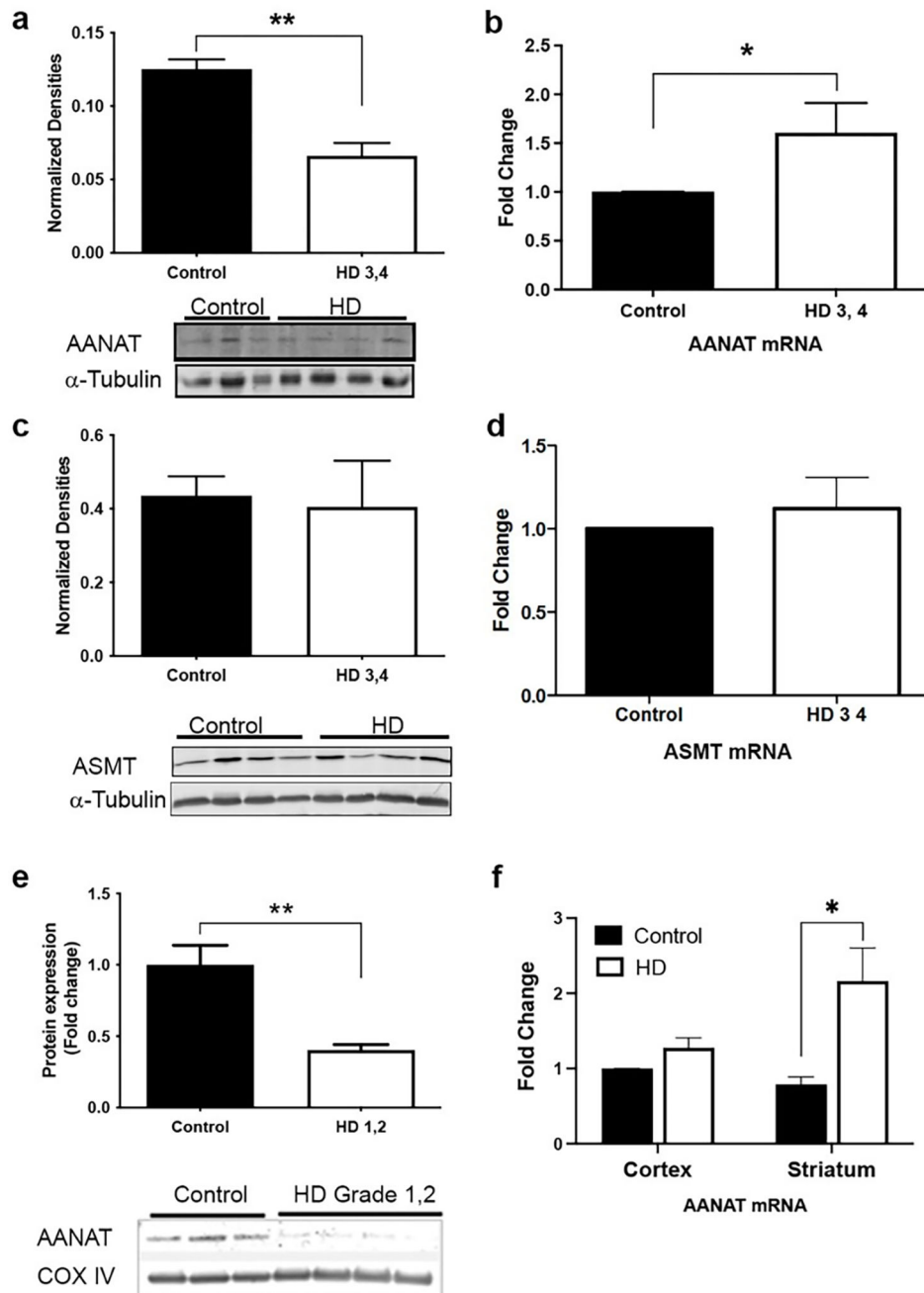


Figure 1.

AANAT protein and *AANAT* mRNA expression in pineal and extrapineal brain tissues of HD patients. **A**, Although AANAT protein expression is decreased in the pineal gland of grade 3–4 HD patients (HD n=4, WT n=3), **B**, *AANAT* mRNA expression is increased in the pineal gland (n=6), compared to control subjects (n=7 [protein], n=3 [mRNA]). **C**, There are no differences in expression of *ASMT* protein (HD n=4, control n=3) or **D**, mRNA (HD n=5, control n=3) in the pineal gland between grade 3–4 HD patients and controls. **E**, AANAT protein expression is decreased in striatal mitochondrial lysates of grade 1–2 HD patients (n=4) compared to controls (n=3). **F**, *AANAT* mRNA expression is increased in

striatal (n = 5), but not cortical (n = 5), mitochondrial samples from grade 3–4 HD patients compared to controls (n = 4 [striatal], 4 [cortical]). * P<0.05, ** P<0.01.

Author Manuscript

Author Manuscript

Author Manuscript

Author Manuscript

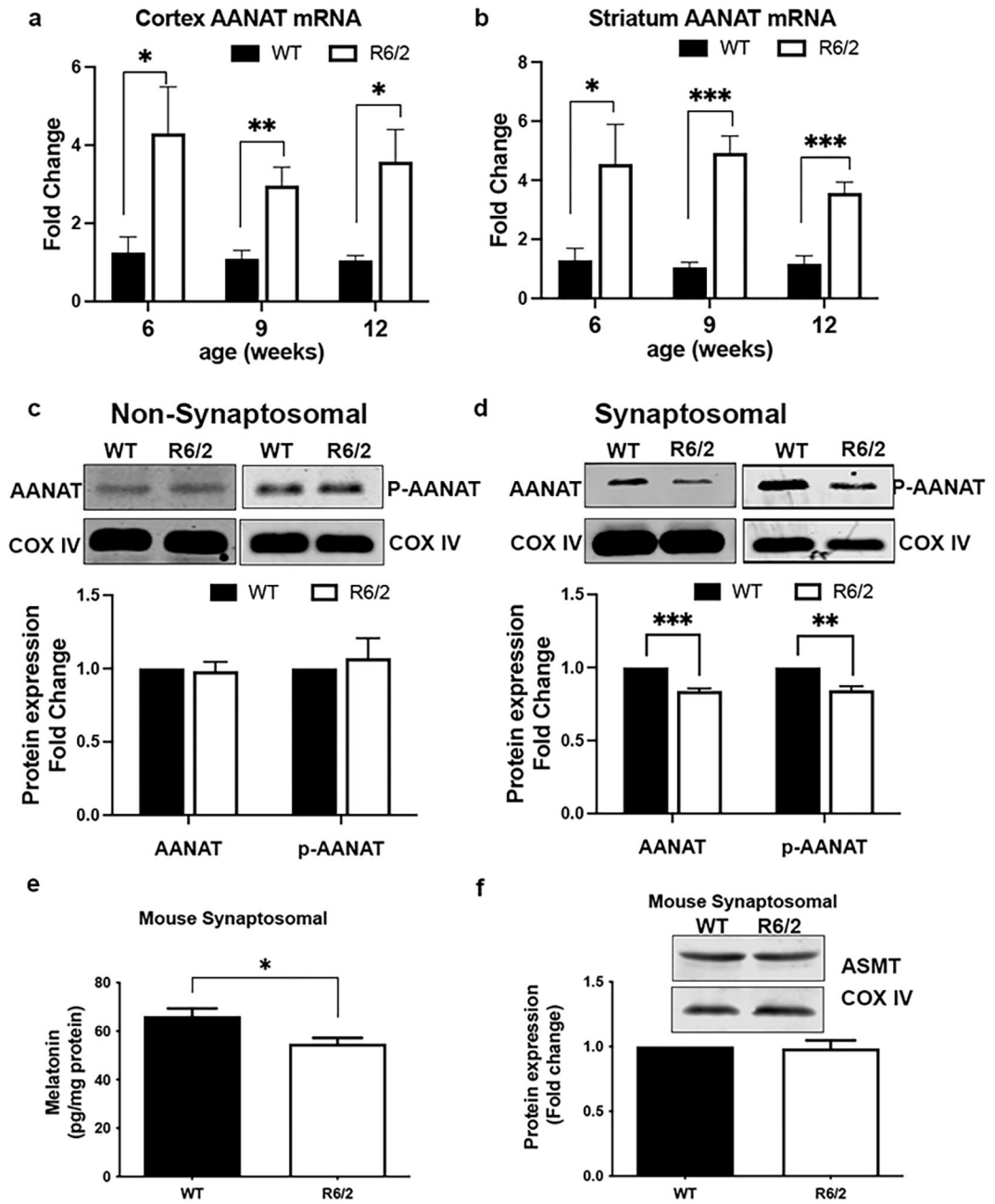


Figure 2.

Extrapineal brain *AANAT* mRNA expression in the R6/2 mouse model of HD. **A**, *AANAT* mRNA expression is increased in the cortex of R6/2 mice at 6, 9, and 12 weeks old (n = 5, 5, 7) compared to WT mice (n = 5, 5, 7). **B**, *AANAT* mRNA expression is increased in the striatum of R6/2 mice at 6, 9, and 12 weeks old (n = 5, 5, 7) compared to WT mice (n = 5, 5, 7). *AANAT* mRNA expression is expressed as fold change relative to WT expression for each time point. **C**, In non-synaptosomal mitochondria of whole forebrain samples, *AANAT* and phospho-*AANAT* expression in 3–4 week old R6/2 mice (n = 3, 3) is not different compared to WT mice (n = 3, 3). **D**, In synaptosomal mitochondria, *AANAT*

and phospho-AANAT expression is decreased in R6/2 mice (n = 3, 3) compared to WT mice (n = 3, 3). **E**, In synaptosomal mitochondria, melatonin expression is decreased in 3–4 week old R6/2 mice (n = 3) compared to WT mice (n = 3). **F**, In synaptosomal mitochondria, ASMT expression in 11–12 week old R6/2 mice (n = 3) is not different compared to WT mice (n = 3). Mitochondria were pooled from four mice of the same genotype per experiment. Densitometry results are presented relative to WT results. * P<0.05, ** P<0.01, *** P<0.001.

Author Manuscript

Author Manuscript

Author Manuscript

Author Manuscript

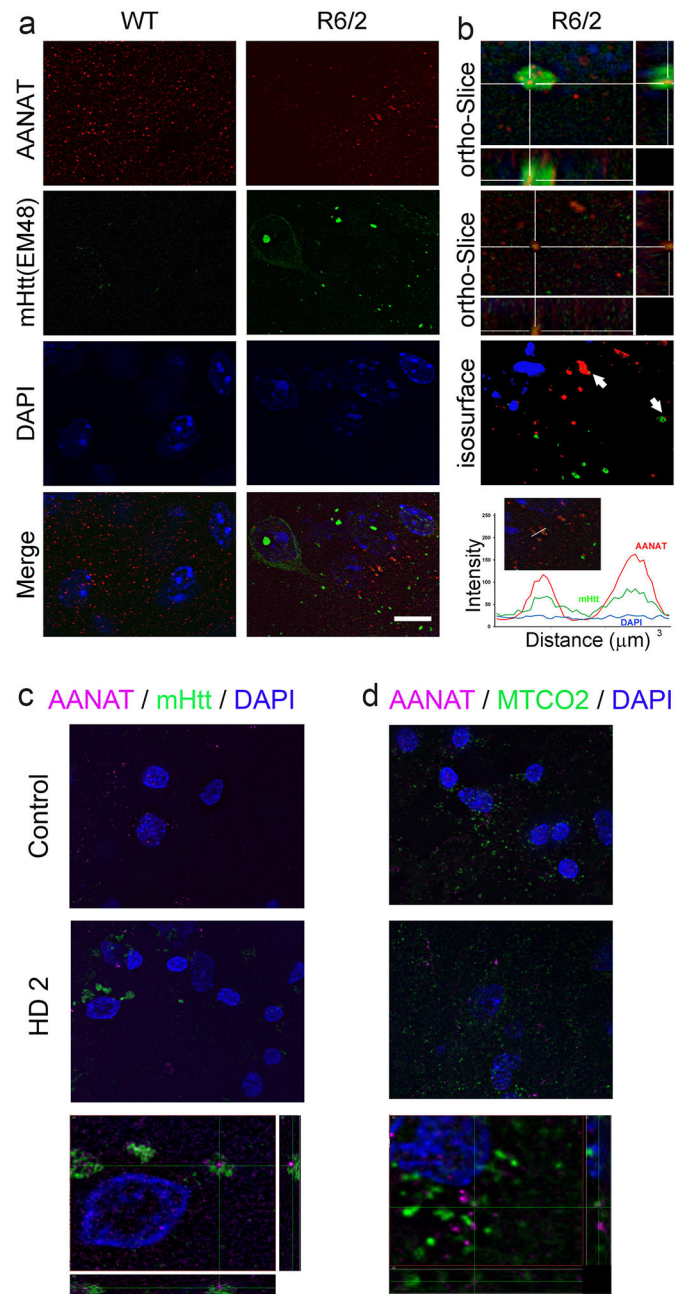


Figure 3. AANAT protein is sequestered in mHTT aggregates in the striatum of R6/2 mice. **A**, Immunohistochemistry of striatal sections from 12 weeks old R6/2 and WT mice for AANAT protein, mHTT protein, and DAPI staining of the nucleus. The anti-Htt EM48 antibody preferentially detects aggregated HTT. **B**, 3D deconvolutional digital images show that mHTT aggregates colocalize with AANAT. Bar = 10 μm . Detailed ortho-Slice, isosurface and line profile analysis of deconvoluted confocal images confirm that mHTT aggregates colocalize with AANAT. **C**, AANAT protein is sequestered in mHTT aggregates in the striatum of human HD patients (representative image, n=3). 3D deconvolutional

digital images and ortho-Slice show mHTT aggregates colocalize with AANAT. **D**, AANAT colocalize with mitochondrial complex 2 (MTCO2) in human striatum.

Author Manuscript

Author Manuscript

Author Manuscript

Author Manuscript

Table 1:

Human specimen information

Type	HD Grade	Specimen	Age	Gender	CAG repeat	Standard brain block (SBB) ^I	Cold PMI	Frozen PMI
Cortex								
Control	n.a	T-99	44	M	N.E.	SBB3.1	23:10	49:15
Control	n.a	T-159	54	F	N.E.	SBB3.1	3:40	15:40
Control	n.a	T-206	49	M	N.E.	SBB3.1	13:55	15:05
Control	n.a	T-343	62	M	N.E.	SBB3.1	4:16	8:16
Control	n.a	T-52	80	M	N.E.	SBB16	N/A	N/A
Control	n.a	T-319	28	F	N.E.	SBB16	2:09	25:34
Control	n.a	T-3962	89	M	N.E.	SBB16	4:47	15:32
HD1	1/4	T-272	83	F		SBB3.1	15:10	16:55
HD1	1/4	T-1146	69	M		SBB3.1	0:08	39:00
HD2	2/4	T-273	67	M		SBB3.1	6:30	32:35
HD2	2/4	T-3221	58	M	42/15	SBB3.1	0:26	85:11
HD2	2/4	T-3049	72	M	43/18	SBB16	15:30	40:50
HD2	2/4	T-4127	50	M	44/28	SBB16	1:00	33:45
HD2	2/4	T-4870	44	M	49/17	SBB16	0:00	39:55
HD3	3/4	T-1905	24	M	71/20	SBB16	5:35	24:21
HD3	3/4	T-1991	53	M	46/17	SBB16	6:45	11:17
HD3	3/4	T-2019	61	M	43/19	SBB16	17:05	18:25
HD3	3/4	T-4495	53	M	40/17	SBB16	1:20	27:35
HD3	3/4	T-4921	47	M	46/20	SBB16	0:00	34:45
Striatum								
Control	n.a	T-99	44	M	N.E.	SBB7.1	23:10	49:15
Control	n.a	T-206	49	M	N.E.	SBB7.1	13:55	15:05
Control	n.a	T-159	54	F	N.E.	SBB7.2	3:40	15:40
Control	n.a	T-52	80	M	N.E.	SBB7	N/A	N/A
Control	n.a	T-110	62	M	N.E.	SBB7	N/A	N/A
Control	n.a	T-111	33	F	N.E.	SBB7	3:40	34:50
HD1	1/4	T-272	83	F		SBB7.1	15:10	16:55
HD1	1/4	T-1146	69	M		SBB7.1	0:08	39:00
HD2	2/4	T-273	67	M		SBB7.0	6:30	32:35
HD2	2/4	T-3221	58	M	42/15	SBB7.0	0:26	85:11
HD2	2/4	T-3049	72	M	43/18	SBB7.1	15:30	40:50
HD2	2/4	T-4127	50	M	44/28	SBB7.4	1:00	33:45
HD3	3/4	T-1905	24	M	71/20	SBB7.1	5:35	24:21
HD3	3/4	T-2019	61	M	43/19	SBB7.2	17:05	18:25

Type	HD Grade	Specimen	Age	Gender	CAG repeat	Standard brain block (SBB) ¹	Cold PMI	Frozen PMI
HD3	3/4	T-1991	53	M	46/17	SBB7	6:45	11:17
HD3	3/4	T-4921	47	M	46/20	SBB7.1	0:00	34:45
HD4	4/4	T-3970	47	F	54/17	SBB7.2	3:30	5:00
HD4	4/4	T-225	72	F	42/19	SBB7	17:55	43:20
Pineal gland								
Control	n.a	T-3966	89	M	N.E.	PIN.0	3:00	15:13
Control	n.a	T-4210	87	M	N.E.	PIN.0	3:12	18:32
Control	n.a	T-111	33	F	N.E.	PIN.0	3:40	34:50
Control	n.a	T-136	64	F	N.E.	PIN.0	7:50	11:30
Control	n.a	T-3998	77	M	N.E.	PIN.0	3:10	33:28
Control	n.a	T-148	66	M	N.E.	PIN.0	10:25	21:55
Control	n.a	T-99	44	M	N.E.	PIN.0	23:10	49:15
Control	n.a	T-159	54	F	N.E.	PIN.0	3:40	15:40
HD3	3/4	T-113	80	M		PIN.0	2:45	4:55
HD3	3/4	T-4091	46	M		PIN.0	0:05	34:16
HD3	3/4	T-2019	61	M	43/19	PIN.0	17:05	18:25
HD3	3/4	T-3430	60	M		PIN.0	5:25	17:55
HD3	3/4	T-2959	47	M		PIN.0	2:20	11:40
HD3	3/4	T-1960	65	F		PIN.0	6:35	18:20
HD4	4/4	T-310	49	F		PIN.0	7:00	8:30
HD4	4/4	T-150	60	M		PIN.0	10:25	12:45
HD4	4/4	T-3960	53	M		PIN.0	11:15	12:50
HD4	4/4	T-260	41	M		PIN.0	2:40	18:55
HD4	4/4	T-291	55	F		PIN.0	3:25	12:25
HD4	4/4	T-3970	47	F	54/17	PIN.0	3:30	5:00
HD4	4/4	T-91	63	M		PIN.0		14:55

Note

Grade - diagnosed HD grade, Specimen - frozen tissue samples, Age - years at death, F - female, M - male, N.E. - not estimated, n.a. - not applicable, CAG repeats - number of CAG repeats of both alleles.

¹Vonsattel, J. P., Del Amaya, M. P. & Keller, C. E. Twenty-first century brain banking. Processing brains for research: the Columbia University methods. *Acta Neuropathol* **115**, 509– 532, doi:10.1007/s00401-007-0311-9 (2008).

Abbreviations

Huntington's disease (HD), amyotrophic lateral sclerosis (ALS), Alzheimer Disease (AD), Parkinson's Disease (PD), multiple sclerosis (MS), mutant-huntingtin (mHTT), aralkylamine N-acetyltransferase (AANAT), acetylserotonin O-methyltransferase (ASMT).